Dalton
Transactions

COMMUNICATION

View Article Online
View Journal | View Issue

Cite this: *Dalton Trans.*, 2025, **54**, 15705

Received 1st September 2025,
Accepted 3rd October 2025

DOI: 10.1039/d5dt02099a

rsc.li/dalton

Catalytic olefin hydrosilylation with an original bis(iminophosphorane)phosphine NPN Co^{II} complex

Ingrid Popovici, Yujia Chen, Sophie Bourcier, Nicolas Casaretto and Audrey Auffrant *

An original bis(iminophosphorane)phosphine NPN ligand was synthesised and coordinated to Co^{II}. Both the ligand and the complex were characterised by multinuclear NMR spectroscopy and X-ray crystallography. The Co^{II} complex (1.5 mol%) in the presence of NaOMe (3 mol%) catalyses the hydrosilylation of olefins within a few hours at 60 °C. Both 1-alkenes and less reactive internal ones built upon a norbornene skeleton were efficiently transformed.

Hydrosilylation of alkenes is of utmost importance for the blooming organosilicon industry.[1,2] Most of the commonly used catalysts incorporate Pt[3] such as the Speier's[4] and Karstedt's[5] complexes. They exhibit good activity and high selectivity in favour of terminal alkylsilanes. However, the high price and limited availability of this precious metal have prompted the search for alternative catalysts that employed more abundant metals. As early as in the 1950s and 1960s, it was demonstrated that iron,[6] cobalt,[7] and nickel[8] salts or their carbonyl derivatives ($[M(CO)_n]$) could catalyse hydrosilylation reactions. However, the incorporation of polydentate ligands has allowed the functional group tolerance to be improved and the reaction conditions to be milder. Ni, Fe and Co olefin hydrosilylation catalysts have been reviewed.[9–15] Most examples are efficient with 1-alkenes, while the conversion of disubstituted olefins is much more difficult to achieve. Examples involving Ni[16–18] and Fe[19] have been reported. Regarding cobalt catalysts, only three examples were catalytically active for such substrates at a temperature between 50 to 80 °C (Scheme 1a). Nagashima reported in 2016 the conversion of some disubstituted olefins with a Co^{II} carboxylate in the presence of isocyanide at 80 °C within a few hours with a loading of 1 mol%.[20] Deng used a NHC Co^{II} precatalyst shown to transform into a Co^{I} active species that realises the hydrosilylation of norbornene within 12 h at 60 °C and a range of 1-alkenes within 1 day at room temperature.[21] Lastly, Nagashima described in 2018 an isocyanide Co^{0} complex[22] that transforms norbornene, cyclopentene, and cyclohexene within 1 day at 50 °C (1 mol%). These examples show the difficulty of converting internal olefins, but also the lack of attention paid to such poorly reactive substrates. Noteworthily, these Co catalysts all feature electron rich ligands (isocyanides or NHC). Iminophosphoranes represent a class of electron-rich N-based ligands[23–25] that have been scarcely employed to develop catalysts. In particular, few iminophosphorane cobalt complexes have been reported for ethene polymerisation,[26] N_2 conversion to $N(SiMe_3)_3$,[27] and olefin hydrosilylation[28]

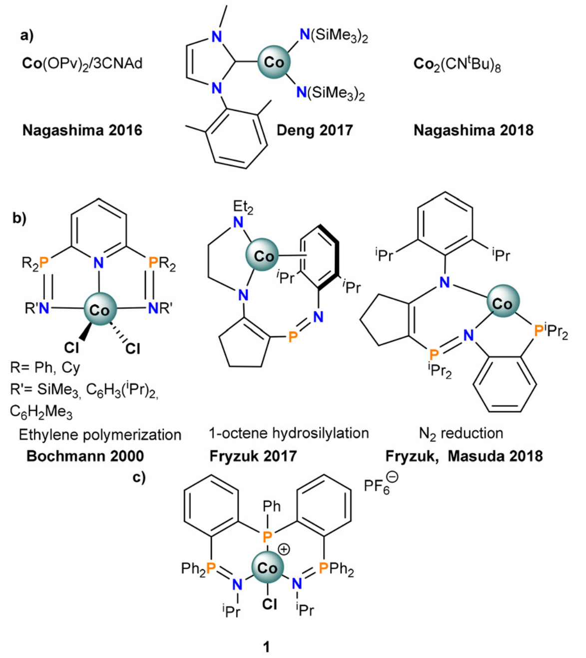

Scheme 1 (a) Cobalt catalysts for the hydrosilylation of internal olefins, (b) previous examples of iminophosphorane Co catalysts, and (c) targeted complex.

Laboratoire de Chimie Moléculaire (LCM), CNRS, Ecole Polytechnique, Institut Polytechnique de Paris, Route de Saclay, 91120 Palaiseau, France. E-mail: audrey.auffrant@polytechnique.edu

(Scheme 1b). In the latter example, a series of NNN–Co^{II} compounds showed a modest catalytic ability for the hydrosilylation of 1-hexene (51% with a 0.5 mol% catalyst loading after 24 h at 50 °C). Based on the idea that the presence of two iminophosphoranes connected to the Co^{II} centre may increase its reactivity in hydrosilylation reactions, we designed an original bis(iminophosphorane) phosphine ligand. Here, we report on the synthesis of this ligand **L** and its Co^{II} complex (**1**), as well as the catalytic performance of the complex in the hydrosilylation of olefins.

For the ligand (**L**) synthesis (Scheme 2), we relied on the *ortho*-lithiation/electrophilic trapping sequence we previously devised in our laboratory.[29,30] The reaction was monitored by *in situ* $^{31}P\{^1H\}$ NMR spectroscopy. Upon addition of two equivalents of ^{n}BuLi in THF, the chosen *N*-isopropyl substituted aminophosphonium led selectively to the *o*-aryllithium adduct characterised by a singlet ^{31}P resonance at 20 ppm. It was directly converted to the NPN ligand upon addition of a half equivalent of $PhPCl_2$. After 3 h, the reaction was finished as shown by the presence of two singlets in a 2 : 1 ratio at −0.4 and −15.5 ppm corresponding respectively to the P^{V} and P^{III} atoms. During the process equivalents of lithium salts were generated. At this stage, it proved difficult to efficiently remove them; repeated washings led to an incomplete elimination. Therefore, we chose to carry out the metalation and then proceed to anion exchange and salt elimination. **LLi_2BrCl** was isolated in 73% yield and characterised by multinuclear NMR spectroscopy and HR-MS.

Single crystals of **L** were grown by diffusion of pentane in a saturated THF solution (Fig. 1A). The ligand exhibits a zig-zag structure in which the two P═N bonds form an angle of 110.7°. They are of similar lengths (1.5481(12) and 1.5695(13) Å) and typical of iminophosphorane derivatives.[31] Coordination of **L** to $CoCl_2$ was realised in THF. $^{31}P\{^1H\}$ NMR monitoring of the crude mixture showed the loss of the P resonances because of the paramagnetism of the formed Co^{II} adduct. Complex **1** was isolated as a bright green solid in 74% yield after ligand exchange with KPF_6 and washing with THF and Et_2O solutions. It was characterised by ^1H NMR spectroscopy, HR-MS, and elemental analysis. Its magnetic moment was measured in solution at 4.31 μ_B corresponding to a total spin of 3/2.[32,33] This value is almost identical to those we recently reported for NNN iminophosphorane Co^{II} complexes.[34] Single crystals of **1** were grown by diffusion of pentane into a concentrated dichloromethane solution. The obtained structure is shown in Fig. 1B. A partial exchange between chloride and bromide was observed (Cl : Br = 76/24). In **1**, the cationic cobalt centre is coordinated to **L** in a κ^3 mode and to the halide. It presents a tetrahedral geometry (τ_4 = 0.99).[35] Both P–N bonds exhibit similar lengths; they are slightly longer than in **L** (~1.61 Å) which is related to the reduced negative hyperconjugation from N to P due to coordination. There is a slight difference in the Co–N bond lengths, Co1–N2 being slightly longer than Co1–N1. Both are longer than those reported by Masuda and Fryzuk for the PNN cobalt(II) complex precursor of the Co^{I} catalyst shown in

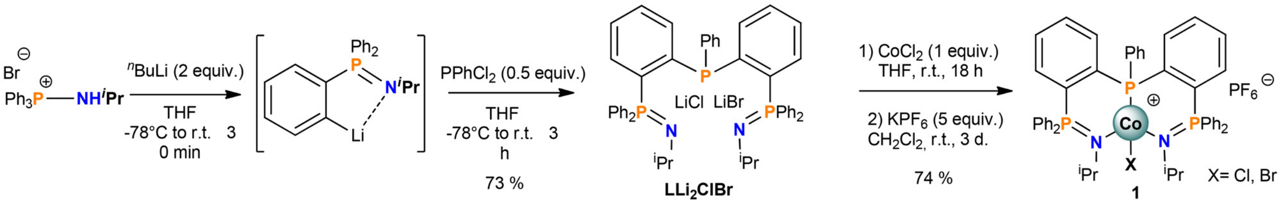

Scheme 2 Synthesis of NPN ligand **L** and complex **1**.

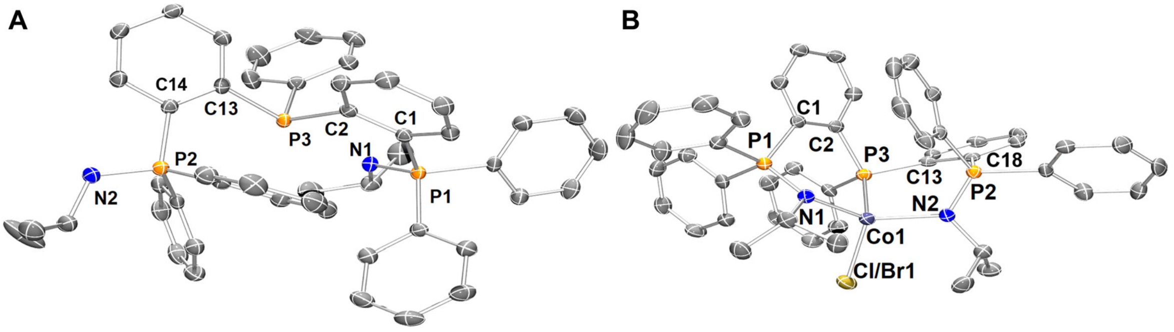

Fig. 1 ORTEP plot of **L** (A) and **1** (B). Hydrogen atoms and the counter anion were omitted for clarity. Thermal ellipsoids were drawn at a 50% probability level. Selected bond lengths (Å) and angles (°): **L** P1–N1 1.5481(12), P2–N2 1.5695(13) P1–C1 1.8061(15), P2–C14 1.8252(15), P3–C2 1.8604(15), P3–C13 1.8679(15), N1–P1–C1 107.54(7), C2–C1–P1 123.44(11), C1–C2–P3 122.15(11), C2–P3–C13 101.27(6), C14–C13–P3 121.48, N2–P2–C14 106.79(7); **1** P1–N1 1.619(2), P2–N2 1.610(5), P3–Co1 2.3600(9), N1–Co1 1.973(2), N2–Co1 2.018(2), P3–C13 1.834(3), P3–C2 1.840(3), N1–Co1–P3 98.46(7), N2–Co1–P3 99.81(7), N1–P1–C1 113.09(13), N2–P2–C18 115.58(12), P1–N1–Co1 123.62(13), P2–N2–Co1 115.28(14).

Scheme 1b.[27] The Co–P bond length is also longer compared to the same reference (2.3600(9) *vs.* 2.3270(8) Å) which denotes a looser coordination of the phosphine to the Co^{II} centre. Because of the formation of the metallacycle, the P3–C2 and P3–C13 bonds are shortened compared to the free ligand.

The catalytic ability of **1** for olefin hydrosilylation was investigated. Transformation of internal olefins was first targeted because of the few efficient Co catalysts reported for such substrates. The optimisation study was thus conducted with norbornene (Table 1). The conversion and yield were determined by ^1H NMR spectroscopy, using trimethoxybenzene as the internal reference. The reaction was initially conducted in THF at 25 °C (concentration 2 M) with one equivalent of silane, 1.5 mol% of **1**, and 3 mol% of sodium methoxide as an additive (Table 1, entry 1). We were pleased to observe the formation of the silane in 65% yield within 6 h. Heating the reaction mixture at 60 °C led to an improved NMR yield of 71% (entry 2). Substituting THF with toluene as the solvent led to a comparable NMR yield (entry 3). Changing for acetonitrile was detrimental (Table S2, entry 1). Upon heating the reaction mixture in toluene to 110 °C, an excellent yield of 90% was obtained (entry 4). However, at 60 °C in THF at a higher concentration (3 M) the yield was even better (98%, entry 5). Using THF (3 M) at 60 °C, the nature of the additive was then modified (Table 1, entries 6–10). The reaction was less efficient with most of the additives tested (sodium isopropoxide, potassium triethylborohydride, cesium carbonate); only potassium *tert*-butoxide and ammonia borane gave excellent yields (88 and 92% respectively) but lower than sodium methoxide. Moreover, changing the amount of this additive only marginally impacted the yield (Table S2, entries 2 and 3), so the study was continued with 3 mol%. Finally, the nature of the silane was changed, only silanes less expensive than Ph_2SiH_2 (polymethylhydrosiloxane (PMHS) and triethoxysilane) were evaluated. Very low conversions were observed in these cases (entries 11 and 12). Having established the optimal conditions (Table 1, entry 5), we verified that the reaction does not proceed in the absence of the catalyst, additive, or ligand (Table S2, entries 4–7). With the established conditions (Table 1, entry 5), we examined the scope of olefins (Scheme 3). Internal olefins with a norbornene scaffold were efficiently converted into the corresponding silanes (**3a–d**). **3a** exhibits only one doublet corresponding to the SiH proton in its ^1H NMR spectrum, showing the selective formation of the

Table 1 Optimisation of the hydrosilylation reaction conditions[a] with the optimised conditions in bold

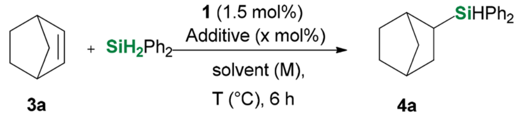

	Si–H	Solv. (x M)	T (°C)	Additive (mol%)	Conv.[b] (%)	Yield[c] (%)
1	Ph_2SiH_2	THF (2)	25	NaOMe (3)	66	65
2	Ph_2SiH_2	THF (2)	60	NaOMe (3)	71	71
3	Ph_2SiH_2	Tol (2)	60	NaOMe (3)	67	67
4	Ph_2SiH_2	Tol (2)	110	NaOMe (3)	92	90
5	**Ph_2SiH_2**	**THF (3)**	**60**	**NaOMe (3)**	**98**	**98**
6	Ph_2SiH_2	THF (3)	60	NaO^iPr (3)	80	80
7	Ph_2SiH_2	THF (3)	60	^tBuOK (3)	88	88
8	Ph_2SiH_2	THF (3)	60	Cs_2CO_3 (3)	25	24
9	Ph_2SiH_2	THF (3)	60	$KHBEt_3$ (1.5)	20	20
10	Ph_2SiH_2	THF (3)	60	NH_3BH_3 (3)	92	92
11	PMHS	THF (3)	60	NaOMe (3)	5	[d]
12	$SiH(OEt)_3$	THF (3)	60	NaOMe (3)	7	[d]

[a] Reaction conducted with norbornene (1 mmol) in the presence of **1**, trimethoxybenzene (0.07 mmol) as the reference, silane (1 mmol) and additive for 6 h. [b] Determined by NMR by using the integration of the singlet at 4.92 ppm for SiH_2Ph_2 relative to the CH aromatic resonances of the reference at 6.10 ppm. [c] Determined by NMR by using the integration of the doublet at 4.72 ppm for $C_6H_{11}SiHPh_2$ relative to the CH aromatic resonances of the reference at 6.10 ppm. [d] Yield could not be determined.

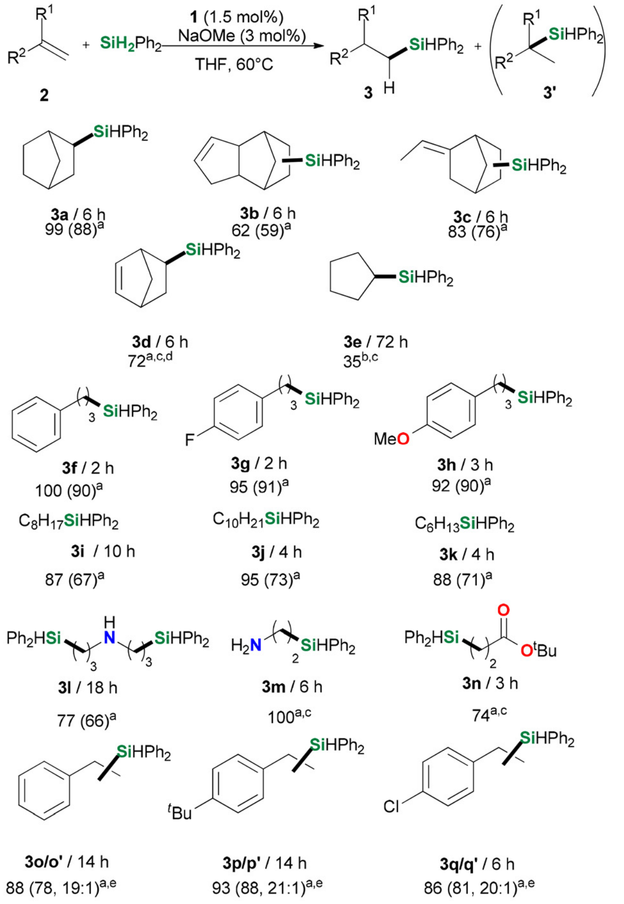

Scheme 3 Scope of the catalytic hydrosilylation of olefins with **1**. NMR yield using trimethoxybenzene as the internal reference is given with the isolated yield specified into brackets. [a] Reaction conducted with the olefin (1 mmol) in the presence of **1** (0.015 mmol, 1.5 mol%), trimethoxybenzene (0.07 mmol) as the reference, SiH_2Ph_2 (1 mmol) and NaOMe (0.03 mmol, 3 mol%) for the specified time at 60 °C in THF (3 M). [b] The same conditions but with **1** (0.03 mmol, 3 mol%) and NaOMe (0.06 mmol, 6 mol%). [c] The product could not be isolated. [d] The NMR conversion is 100% and side products are also formed. [e] NMR yield and isolated yield correspond to the mixture of linear (**4**) and branched (**4'**) products (**4** : **4'**).

exo adduct. For **3d**, four doublet SiH resonances were observed by ^{1}H NMR; but the major one at 4.82 ppm corresponds to the *exo* product that forms in 72% yield (the three other silanes being formed in a global yield of 28%). Note that the hydrosilylation of norbornene with low valent Co catalysts was not as selective, because the *endo* product was also observed.[22] For **3b** and **3c** two doublet resonances corresponding two different SiH protons were observed, pointing towards the formation of both regioisomers that could not be separated. The hydrosilylation of cyclopentene (**2e**), cyclohexene, or *gem*-disubstituted olefins (Scheme S1) proved more difficult. Increasing the catalyst loading and/or extending the reaction time led to minor improvements. Only **3e** was formed in 35% yield with 3 mol% catalyst after 3 days. Then we evaluated the catalytic capacity of **1** with terminal olefins. Linear aliphatic silanes formed selectively and efficiently. Allylbenzene derivatives were converted in excellent yields within 2 or 3 h. In the presence of a donating substituent *para* to the allyl group (**2h**), the reaction was only marginally less rapid and efficient than when an acceptor substituent was present (**2g**).

For a longer alkyl chain, hexene and decene (**2j–k**) were more reactive than octene (**2i**); a NMR yield around 90% required only 4 h from the former compared to 10 h from the latter. Note that low valent cobalt catalysts previously mentioned[20–22] are generally less efficient for this type of substrate or require a longer reaction time to reach good yields because of competitive alkene isomerisation and dehydrogenative silylation. For **1**, a good functional group compatibility was observed: amine, ester, ether, and halide were well tolerated. However, cinnamonitrile was not converted (Scheme S1) presumably because of the poisoning effect of the nitrile onto the catalyst. Lastly, styrene derivatives (**3o–q**) were converted in high yield and excellent selectivity into the linear silane products (>94%).

The performances of complex **1** regarding the hydrosilylation of norbornene derivatives are remarkable for such a cobalt(II) complex with a rather rigid tridentate ligand. Therefore, we verified that the process is homogeneous by conducting the hydrosilylation of norbornene in the presence of a mercury drop. The expected silane was obtained in 89% yield (Fig. S10).

In conclusion, the cobalt complex **1** with an original NPN bis(iminophosphorane)phosphine ligand was shown to be an excellent catalyst for the hydrosilylation of olefins. Terminal olefins were efficiently and selectively converted. Styrene derivatives were also hydrosilylated with high selectivity. But the most astonishing performance concerns norbornene scaffolds. Such catalytic ability is unprecedented with a cobalt (II) complex and encourages us to continue exploring other catalytic reactions.

Author contributions

I. P.: formal analysis, data curation, investigation, and writing of the original draft. Y. C.: investigation. S. B.: formal analysis and data curation. N. C.: formal analysis and data curation. A. A.: formal analysis, funding acquisition, data curation, and writing of the original draft.

Conflicts of interest

There are no conflicts to declare.

Data availability

CCDC 2477583 and 2477584 contain the supplementary crystallographic data for this paper.[36a,b]

Details concerning syntheses, catalytic experiments as well as NMR data are provided as supplementary information (SI). Supplementary information is available. See DOI: **https://doi.org/10.1039/d5dt02099a**.

Acknowledgements

This work was supported by the CNRS, Ecole Polytechnique, and the Agence Nationale de la Recherche (ANR21-CE07-0026).

References

1 Y. Nakajima and S. Shimada, *RSC Adv.*, 2015, **5**, 20603–20616.

2 B. Marciniec, H. Maciejewski, C. Pietraszuk and P. Pawluc, *Hydrosilylation A Comprehensive Review on Recent Advances*, Springer, Ntelns, 2009.

3 Y. Naganawa, K. Inomata, K. Sato and Y. Nakajima, *Tetrahedron Lett.*, 2020, **61**, 151513.

4 J. L. Speier, J. A. Webster and G. H. Barnes, *J. Am. Chem. Soc.*, 1957, **79**, 974–979.

5 (*a*) B. D. Karstedt, *US pat.*, US3775452A, General Electric Company, 1973; (*b*) D. Troegel and J. Stohrer, *Coord. Chem. Rev.*, 2011, **255**, 1440–1459.

6 A. J. Chalk and J. F. Harrod, *J. Am. Chem. Soc.*, 1965, **87**, 1133–1135.

7 A. N. Nesmeyanov, R. K. Freidlina, E. C. Chukovskaya, R. G. Petrova and A. B. Belyavsky, *Tetrahedron*, 1962, **17**, 61–68.

8 S. I. Nozakura, *Bull. Chem. Soc. Jpn*, 1956, **29**, 784–789.

9 M. Zhang and A. Zhang, *Appl. Organomet. Chem.*, 2010, **24**, 751–757.

10 J. Sun and L. Deng, *ACS Catal.*, 2016, **6**, 290–300.

11 X. Du and Z. Huang, *ACS Catal.*, 2017, **7**, 1227–1243.

12 J. V. Obligacion and P. J. Chirik, *Nat. Rev. Chem.*, 2018, **2**, 15–34.

13 W. Ai, R. Zhong, X. Liu and Q. Liu, *Chem. Rev.*, 2019, **119**, 2876–2953.

14 H. Wen, G. Liu and Z. Huang, *Coord. Chem. Rev.*, 2019, **386**, 138–153.

15 J. Jose and T. V. Mathew, *ChemCatChem*, 2024, **16**, e202301626.

16 I. Buslov, J. Becouse, S. Mazza, M. Montandon-Clerc and X. Hu, *Angew. Chem., Int. Ed.*, 2015, **54**, 14523–14526.

17 I. Hossain and J. A. R. Schmidt, *Organometallics*, 2020, **39**, 3441–3451.

18 V. Srinivas, Y. Nakajima, W. Ando, K. Sato and S. Shimada, *Catal. Sci. Technol.*, 2015, **5**, 2081–2084.

19 J. Chen, B. Cheng, M. Cao and Z. Lu, *Angew. Chem., Int. Ed.*, 2015, **54**, 4661–4664.

20 D. Noda, A. Tahara, Y. Sunada and H. Nagashima, *J. Am. Chem. Soc.*, 2016, **138**, 2480–2483.

21 Y. Liu and L. Deng, *J. Am. Chem. Soc.*, 2017, **139**, 1798–1801.

22 A. Sanagawa and H. Nagashima, *Organometallics*, 2018, **37**, 2859–2871.

23 T. Tannoux and A. Auffrant, *Coord. Chem. Rev.*, 2023, **474**, 214845.

24 I. Popovici, C. Barthes, T. Tannoux, C. Duhayon, N. Casaretto, A. Monari, A. Auffrant and Y. Canac, *Inorg. Chem.*, 2023, **62**, 2376–2388.

25 S. E. García-Garrido, A. Presa Soto and J. García-Álvarez, in *Advances in Organometallic Chemistry*, ed. P. J. Pérez, Academic Press, 2022, pp. 105–168.

26 S. Al-Benna, M. J. Sarsfield, M. Thornton-Pett, D. L. Ormsby, P. J. Maddox, P. Brès and M. Bochmann, *J. Chem. Soc., Dalton Trans.*, 2000, 4247–4257.

27 T. Suzuki, K. Fujimoto, Y. Takemoto, Y. Wasada-Tsutsui, T. Ozawa, T. Inomata, M. D. Fryzuk and H. Masuda, *ACS Catal.*, 2018, **8**, 3011–3015.

28 T. Suzuki, H. Masuda and M. D. Fryzuk, *Dalton Trans.*, 2017, **46**, 6612–6622.

29 L. Boubekeur, L. Ricard, N. Mezailles, M. Demange, A. Auffrant and P. Le Floch, *Organometallics*, 2006, **25**, 3091–3094.

30 A. Buchard, A. Auffrant, C. Klemps, L. Vu-Do, L. Boubekeur, X. F. Le Goff and P. Le Floch, *Chem. Commun.*, 2007, 1502–1504.

31 T. Cheisson, L. Ricard, F. W. Heinemann, K. Meyer, A. Auffrant and G. Nocton, *Inorg. Chem.*, 2018, **57**, 9230–9240.

32 D. F. Evans, *J. Chem. Soc., Chem. Commun.*, 1959, 2003–2005.

33 E. M. Schubert, *J. Chem. Educ.*, 1992, **69**, 62.

34 I. Popovici, T. Tannoux, S. Bourcier, N. Casaretto and A. Auffrant, *Inorg. Chem. Commun.*, 2025, **180**, 114917.

35 L. Yang, D. R. Powell and R. P. Houser, *Dalton Trans.*, 2007, 955–964.

36 (*a*) CCDC 2477583: Experimental Crystal Structure Determination, 2025, DOI: **10.5517/ccdc.csd.cc2p5412**; (*b*) CCDC 2477584: Experimental Crystal Structure Determination, 2025, DOI: **10.5517/ccdc.csd.cc2p5423**.